Geophys. J. R. astr. Soc. (1979) **56**, 81–96

Near-field waveforms from an arbitrarily expanding, transparent spherical cavity in a prestressed medium

J. B. Minster *Seismological Laboratory, California Institute of Technology, Pasadena, California 91125, USA*

Received 1978 June 28; in original form 1978 January 1

Summary. A simple, approximate ('transparent') solution is derived for the near-field radiation emitted by a spherical cavity expanding in an initial pure shear prestress field. Near-field terms, their propagation and decay are discussed for a variety of growth histories, and are shown to be rather insensitive to the detailed variations of rupture velocity. The transparency approximation is shown to be adequate in the near field as well as in the far field; the main effect is a slight narrowing of far-field pulses. Time domain moment estimators at close range are more reliable for the *S* wave than for the *P* wave since transverse pulses are not as strongly contaminated by near-field effects.

Introduction

In an earlier paper, Minster & Suteau (1977) investigated the far-field waveforms generated by the progressive creation of a spherical cavity in a prestressed medium. In this paper we investigate the near-field radiation for this source, using the same method of solution. This solution, developed by Archambeau (1968, 1972) and Minster (1973), assumes the source region to be transparent to incident radiation. In other words, it ignores the excitation of free oscillations of the cavity, as pointed out by Burridge (1975). This approximation leads to a simpler, analytical solution, even in the case of non-uniform growth of the cavity. In addition, more complicated situations involving transonic and supersonic rupture velocities may be handled as well.

Whereas numerous studies of this problem – particularly the case of instantaneous creation of the cavity – can be found in the literature (e.g. Randall 1964; Archambeau 1972; Koyama *et al.* 1973), most of these deal exclusively with the far-field radiation. Some investigations of the near-field terms in the spectral domain were conducted by Archambeau (1972), Randall (1973b), Minster (1973) and Burridge (1975). Harkrider (1976) computed time domain near-field solutions for the special case of infinite rupture velocity. Burridge (1975) obtained a non-transparent solution for a piecewise constant, subsonic rupture velocity. Comparison of our results with Burridge's will permit a better assessment of the quality of the 'transparency' approximation.

The radial and tangential components of acceleration are simply related to the potential solution. Numerical integration yields the velocity and displacement components. Properties of the near-field radiation are discussed based on selected numerical examples.

1 Potential solution

We consider a self-similarly expanding spherical cavity in an infinite isotropic elastic medium under uniform, pure shear, prestress. Application of the formal elastodynamic representation theorem, taking into account the presence of the moving boundary, yields an integral equation for the radiated displacement field (Archambeau & Minster 1978, equation 89). Clearly the solution depends on the choice of boundary conditions to be satisfied on the moving boundary. As discussed below in Section 3, this choice is somewhat arbitrary and requires a more complete description of the physical process taking place at the boundary. In this paper, we adopt the transparent solution, which approximates the radiation field by considering only the initial value contribution and ignoring the dynamic interaction of the radiation field and the cavity. This contribution is (e.g. Archambeau & Minster 1978, equation 93)

$$\mathbf{u}(\mathbf{r},t)=\frac{1}{4\pi}\int_0^{\tau} dt_0 \int_{\mathcal{V}(t_0)} \frac{\partial \mathbf{u}^*}{\partial t_0}\cdot\frac{\partial \Gamma^{\mathrm{m}}}{\partial t_0}\,dv^0 \tag{1.1a}$$

where $\mathbf{u}$ is the displacement field, $\mathbf{u}^*$ its initial value, function of the source time t_0, and Γ^{m} is the infinite space Green's tensor. The volume integral is evaluated over the whole space outside the cavity.

In this paper we shall give an exact, analytical evaluation of (1.1a), both in the frequency domain and in the time domain.

Let $\chi_i=\Omega_i$, $i=1, 2, 3$, be the Cartesian components of the rotation potential, and $\chi_4=0$ be the dilatation; let $k_4=\omega/V_p=k_p$; $k_i=\omega/V_s=k_s$ be the compressional and shear wave numbers, then the spectral domain solution in spherical coordinates is (Minster 1973)

$$\tilde{\chi}_\alpha(\mathbf{r},\omega)=C_\alpha(\theta,\phi)\left[h_2^{(2)}(k_\alpha r)k_\alpha^2\tilde{\mathscr{V}}_\alpha-\frac{i}{k_\alpha r^3}\tilde{\mathscr{W}}_\alpha\right],\qquad \alpha=1,\ldots,4, \tag{1.1b}$$

where $C_\alpha(\theta,\phi)$ represents the radiation pattern, $\tilde{\mathscr{V}}_\alpha$ the reduced spectrum and $\tilde{\mathscr{W}}_\alpha$ is a non-radiative term representing the static fields. If $R(t_0)$ is the cavity radius, $V_{\mathrm{R}}(t_0)=\dot{R}(t_0)$ is the rupture velocity and we adopt the convention, appropriate for contained underground explosions (Minster & Suteau 1977)

$$\left.\begin{array}{lll} V_s<V_p\leqslant V_{\mathrm{R}}(t_0) & \text{for} & 0\leqslant t_0<\tau_p,\\ V_s\leqslant V_{\mathrm{R}}(t_0)<V_p & \text{for} & \tau_p<t_0\leqslant\tau_s,\\ V_{\mathrm{R}}(t_0)<V_s<V_p & \text{for} & \tau_s<t_0<\tau,\\ V_{\mathrm{R}}(t_0)=0 & \text{for} & \tau<t_0. \end{array}\right\} \tag{1.2}$$

Let $\tau_i=\tau_s$, $i=1, 2, 3$, and $\tau_4=\tau_p$, then, as shown by Minster & Suteau,

$$\tilde{\mathscr{V}}_\alpha(\omega)=\frac{3}{V_\alpha}\int_0^{\tau}\exp(-i\omega t_0)R^2(t_0)\left[\dot{R}(t_0)H(t_0-\tau_\alpha)+\frac{R(\tau_\alpha)}{3}\delta(t_0-\tau_\alpha)\right]\frac{j_1(k_\alpha R(t_0))}{k_\alpha R(t_0)}\,dt_0. \tag{1.3}$$

Let us denote the bracket in the integrand by $\dot{R}_\alpha(t_0)$. Similarly

$$\tilde{\mathscr{W}}_\alpha(\omega) = \frac{3}{V_\alpha}\int_0^\tau \exp(-i\omega t_0)R^2(t_0)\dot{R}_\alpha(t_0)dt_0, \tag{1.4}$$

where it is assumed that the cavity radius increases semi-monotonically for the solution to be valid (e.g. Minster 1973; Minster & Suteau 1977). Without loss of generality we assume that the pure shear prestress $\sigma_{ij}^{(0)}$ is such that only $\sigma_{13}^{(0)}$ is non-zero. Then (e.g. Harkrider 1977)

$$\left.\begin{aligned}
C_1(\theta,\phi) &= \frac{3K_s\sigma_{13}^{(0)}}{8}\sin 2\phi(1-\cos 2\theta),\\
C_2(\theta,\phi) &= \frac{3K_s\sigma_{13}^{(0)}}{8}(3\cos 2\theta+1) - \frac{3K_s\sigma_{13}^{(0)}}{8}\cos 2\phi(1-\cos 2\theta),\\
C_3(\theta,\phi) &= -\frac{3K_s\sigma_{13}^{(0)}}{4}\sin\phi\sin 2\theta,\\
C_4(\theta,\phi) &= \frac{3K_sV_s^2\sigma_{13}^{(0)}}{V_p^2}\cos\phi\sin 2\theta,
\end{aligned}\right\} \tag{1.5}$$

where $K_s = 5(1-\nu)/\mu(7-5\nu)$; μ is the rigidity, ν Poisson's ratio. The time domain solution is the result of the inverse transformation

$$\chi_\alpha(\mathbf{r},t)\frac{1}{2\pi}\int_{-\infty}^{+\infty}\tilde{\chi}_\alpha(\mathbf{r},\omega)\exp(i\omega t)d\omega. \tag{1.6}$$

Evaluating this integral is straightforward but rather lengthy. This is done in Appendix A and the results may be summarized as follows: let

$$t'_\alpha = t - r/V_\alpha,$$

then

$$\chi_\alpha(\mathbf{r},t) = C_\alpha(\theta,\phi)\int_0^\tau I_\alpha(t_0)dt_0 = C_\alpha(\theta,\phi)F_\alpha(t) \tag{1.7}$$

with

$$F_\alpha(t) = -\frac{3}{4}\left[-\frac{2V_\alpha}{r}J_1 + \frac{3}{r^2}J_2 - \frac{3V_\alpha^2}{r^2}J_3 + \frac{3V_\alpha}{r^3}J_4 - \frac{V_\alpha^3}{r^3}J_5 - \frac{2}{r^3}J_6\right] + \frac{3}{r^3}J_7 - \frac{R_0^3}{r^3}, \tag{1.8}$$

where $R_0 = R(\tau)$ is the final radius.

The quantities J_i are given by the following integrals:

$$J_1 = \int_{T_i}^{T_f}\frac{\dot{R}_\alpha}{R}(t'_\alpha - t_0)dt_0, \tag{1.9}$$

$$J_2 = \int_{T_i}^{T_f}\dot{R}_\alpha R dt_0, \tag{1.10}$$

$$J_3 = \int_{T_i}^{T_f} \frac{\dot{R}_\alpha}{R}(t'_\alpha - t_0)^2 dt_0, \tag{1.11}$$

$$J_4 = \int_{T_i}^{T_f} \dot{R}_\alpha R(t'_\alpha - t_0) dt_0, \tag{1.12}$$

$$J_5 = \int_{T_i}^{T_f} \frac{\dot{R}_\alpha}{R}(t'_\alpha - t_0) dt_0, \tag{1.13}$$

$$J_6 = \int_{T_i}^{T_f} \dot{R}_\alpha R^2 dt_0, \tag{1.14}$$

$$J_7 = \int_{T_f}^{\tau} \dot{R}_\alpha R^2 dt_0. \tag{1.15}$$

The bounds in these integrals are functions of r and t given by

$$\left.\begin{aligned} T_i &= \max(\tau_1, \tau_\alpha), \\ T_f &= \min(\tau_2, \tau), \end{aligned}\right\} \tag{1.16}$$

subject to the constraint $T_i \leqslant T_f$, where

$$\left.\begin{aligned} V_\alpha(t' - \tau_2) + R(\tau_2) &= 0, \\ V_\alpha(t' - \tau_1) - R(\tau_1) &= 0. \end{aligned}\right\} \tag{1.17}$$

When $R(t_0)$ is a quadratic function of t_0, the integrals $J_1, \ldots, J_7$ have closed forms which are given in Appendix B.

Changes in the behaviour of the potential waveform occur at the following reduced times, obtained from the conditions

$$(1)\ \tau_2 = \tau_\alpha, \quad t'_\alpha = \tau_\alpha - \frac{R(\tau_\alpha)}{V_\alpha}, \quad \alpha = p, s,$$

corresponding to the onset of waves leaving from the near side of the cavity at the source time τ_α – i.e. when the rupture velocity falls below the wave speed (phases P, S).

$$(2)\ \tau_2 = \tau, \quad t'_\alpha = \tau - \frac{R(\tau)}{V_\alpha}, \quad \alpha = p, s,$$

which are the stopping phases radiated from the near side of the cavity (phases P_s, S_s).

$$(3)\ \tau_1 = \tau_\alpha, \quad t'_\alpha = \tau_\alpha + \frac{R(\tau_\alpha)}{V_\alpha}, \quad \alpha = p, s,$$

which are the starting phases radiated from the far side of the cavity (phases P', S').

$$(4)\ \tau_1 = \tau, \quad t'_\alpha = \tau + \frac{R(\tau)}{V_\alpha}, \quad \alpha = p, s,$$

which are the stopping phases radiated from the far side of the cavity (phases P'_s, S'_s).

These phases occur both for the P and S waves, and will be more obvious in the velocity pulses than in the displacement waveforms.

2 Accelerations, velocities, displacements

The acceleration vector is obtained from the potentials through the equation

$$\mathbf{a} = V_p^2 \nabla\Theta - 2V_s^2 \nabla\times\ \Omega \tag{2.1}$$

where Θ and Ω are the dilatation and rotation potentials, respectively. Let

$$\left.\begin{aligned}\Theta &= C_4(\theta,\phi)\Theta',\\ \Omega_i &= C_i(\theta,\phi)\Omega',\end{aligned}\right\} \tag{2.2}$$

then the spherical components of acceleration are given by

$$\left.\begin{aligned} a_r &= 3K_s V_s^2 \sigma_{13}^{(0)} \cos\phi \sin 2\theta \left[\frac{\partial\Theta'}{\partial r} + 3\frac{\Omega'}{r}\right],\\ a_\theta &= 3K_s V_s^2 \sigma_{13}^{(0)} \cos\phi \cos 2\theta \left[2\frac{\Theta'}{r} + \frac{\partial\Omega'}{\partial r} + \frac{\Omega'}{r}\right],\\ a_\phi &= -3K_s V_s^2 \sigma_{13}^{(0)} \sin\phi \cos\theta \left[2\frac{\Theta'}{r} + \frac{\partial\Omega'}{\partial r} + \frac{\Omega'}{r}\right].\end{aligned}\right\} \tag{2.3}$$

Thus the acceleration field possesses a double-couple radiation pattern, and depends only on the two functions Θ', Ω' and their radial derivatives. The necessary expressions to calculate these radial derivatives are given in Appendix B. However, because the radial derivatives in (2.3) yield singular terms whenever the rupture velocity equals the wave velocity, time integration to obtain the velocity field involves the evaluation of principal value integrals. The following procedure is therefore preferable: write

$$I_\alpha = \sum_k c_k(r) J_k(t'), \tag{2.4}$$

so that

$$\frac{\partial I_\alpha}{\partial r} = \sum_k \frac{\partial c_k(r)}{\partial r} J_k(t') - \frac{1}{V_\alpha} c_k(r) \frac{\partial J_k(t')}{\partial t'}. \tag{2.5}$$

The first term is non-singular and its quadrature may be performed numerically, whereas the quadrature of the second term may be performed analytically, yielding $-I_\alpha/V_\alpha$. This procedure avoids numerical difficulties in calculating the velocity radiation. An additional quadrature yields the displacement.

Because near-field terms are included in (2.1), one cannot separate the radiation field into P and S waves (Pendse 1948). Whenever one attempts to do so, the P and S amplitude spectra are found to grow as ω^{-3} as $\omega \to 0$. This is equivalent to a parabolic growth in the time domain. Recombination in terms of radial and transverse components yields an ω^{-1} long-period spectral dependence corresponding to the long time static offset (Minster 1973; Burridge 1975). In view of the form of (2.3), one only need compute the radial and transverse time histories, and the radiation pattern appears only as a multiplicative factor.

3 Numerical calculations and discussion

Although the expressions given above only require that $\dot{R}(t_0) \geqslant 0$, for numerical applications, we confine ourselves to quadratic growth histories of the cavity. The far-field

radiation from this model was discussed by Minster & Suteau (1977) and our main concern lies with the near-field behaviour of the waves. Let

$$R(t_0) = \frac{A}{2}(t_0 - z_1)(t_0 - z_2), \tag{3.1}$$

where it is assumed that A is non-positive, and that

$$z_2 \leqslant 0; \quad 2\tau \leqslant z_1 + z_2, \tag{3.2}$$

so that no shrinkage of the cavity is allowed. Following Burridge (1975) we represent the waveforms as functions of a dimensionless time such as tV_s/R_0, and use R_0 as unit of length.

3.1 PROPAGATION AND DECAY OF THE WAVES

Fig. 1 demonstrates the evolution of velocities and displacements with increasing distance from the source. The numerical parameters adopted for the calculations are, in arbitrary but self-consistent units, $V_s = 1$, $V_p = \sqrt{3}$ (Poisson solid), $R_0 = 1$, $V_r = \dot{R} = 0.9\,V_s$. From the discussion of the various phases given earlier, the acceleration pulses for the radial and transverse components are completely distinct if

$$r \geqslant \frac{(V_R + V_p)V_s}{(V_p - V_s)V_R} R_0 = r^*. \tag{3.3}$$

For $r \leqslant r^*$, the velocity pulses are rather complicated, but the displacements have a remarkably simple appearance. Note the conspicuous near-field transverse pulse with a

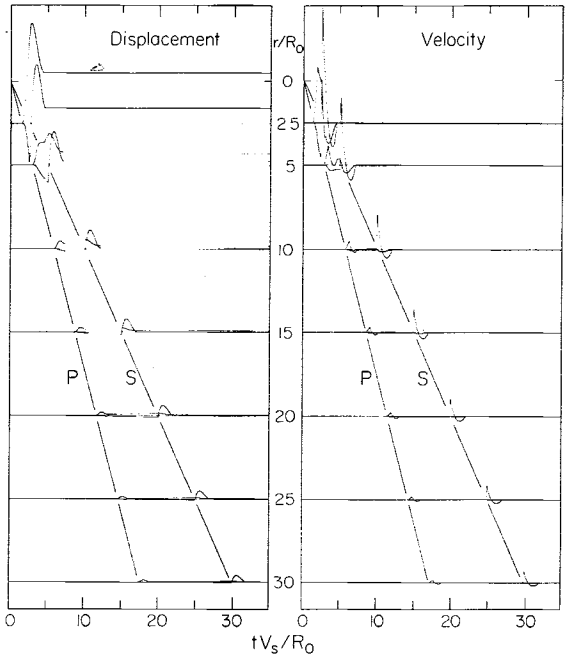

Figure 1. Time–distance plot of near-field velocity and displacement waveforms. Travel-time curves for *S* and *P* waves are also shown. Parameters are given in the text.

polarity opposite to that of the corresponding far-field pulse. It decays rapidly with increasing distance and appears to correspond to a 'Poisson effect' associated with the radial near-field displacement. For $r \geqslant r^*$, the radial and transverse acceleration pulses separate and there exists a time interval during which the velocities grow linearly with time, yielding a slow parabolic growth of the displacement. This is in agreement with the results of Burridge (1975) and Harkrider (1976). The velocity components must vanish after the end of the transverse pulse, so that the integrals of acceleration pulses must be zero. The verification that this is indeed the case (Fig. 1) provides a very powerful check of the correctness of the analytical expressions given in the appendices, and of the accuracy of the numerical calculations.

Another aspect of Fig. 1 concerns the emergence of the far-field radiation at large distances. It stems from the slow decaying terms (r^{-1}) in the solution. It is seen that at distances of 20 or more cavity radii, most of the short-period content of the pulses consists of the far-field terms so that near-field effects will only be seen on long-period detectors. This is consistent with the spectral domain analysis of Minster (1973) and Burridge (1975). Since the far-field approximation is defined by $kr \gg 1$, where k is the wavenumber, it is clearly a better approximation at high frequencies.

Harkrider (1976) developed criteria for estimating the minimum range at which far-field approximations may be used in time domain moment estimates. These critical ranges are:

$$\frac{r_c^{(p)}}{R_0} = \frac{5V_p(3V_p^2 - V_s^2)}{V_s^2} \Delta T_{1/2}^{(p)} \frac{V_s}{R_0}, \tag{3.4}$$

$$\frac{r_c^{(s)}}{R_0} = \frac{10V_s^3}{V_p^2 V_s} \Delta T_{1/2}^{(s)} \frac{V_s}{R_0}. \tag{3.5}$$

Here $\Delta T_{1/2}$ is the pulse width measured at the half-peak amplitude level. For the waveforms of Fig. 1, we find that $r_c^{(p)}$ is of the order of $50R_0$, while $r_c^{(s)}$ is only of the order of $5R_0$. This rather large difference may be explained heuristically by noting that transverse pulses, measured from the S arrival time in Fig. 1, do not undergo drastic changes in shape with increasing distance, while radial pulses evolve rather rapidly.

In the spectral domain, one may define a far-field corner frequency f_c in the usual manner, and a near-field critical frequency f_n at the intersection of the near field ω^{-1} spectral asymptote with the far-field long-period spectral level (e.g. Randall 1973b). Harkrider (1976) compared the Ohnaka (1973) dislocation model and the Randall (1964, 1973a) and Archambeau (1972) relaxation source model. He concluded that the criteria (3.4) and (3.5) led to a spectral criterion $f_c \sim 24.5 f_n$. By considering the same model as used in this paper, and requiring that $f_n \leqslant f_c/10$, Minster (1973) suggested a compromise distance of $r_c \cong 20R(\tau)$ for far-field spectral estimates of the moment. It appears from this discussion that near-field effects are much more likely to contaminate P-wave moment estimates than S-wave moment estimates at short distances. This is confirmed by the observation that the radial components of near-field radiation, including the final static value, are much larger in relation to the P pulse amplitude than the transverse components are to the S pulse amplitude (Fig. 1).

3.2 TRANSPARENT SOURCE AND EXACT SOLUTION

One important question which must be addressed concerns the effect of the 'transparent source' approximation on the calculated radiated field. Our solution ignores waves scattered

by the cavity, as well as free oscillations of the cavity (Archambeau 1968, 1972; Minster 1973; Burridge 1975; Archambeau & Minster 1978). As discussed by Burridge (1976) use of the word 'cavity' introduces a conceptual difficulty since it implies either a violation of mass conservation, or a radial outflow of mass (e.g. Snoke 1976). Since we are only concerned with a pure shear prestress, we shall assume that 'cavity' actually means complete loss of rigidity of the material upon failure, with no density change (e.g. Burridge 1976). The suitable boundary conditions in that case are given by Archambeau & Minster (1978) and reduce to the jump conditions:

$$[\![V_i n_i]\!] = 0, \tag{3.6a}$$

$$[\![t_i]\!] = \rho U [\![V_i]\!], \tag{3.6b}$$

$$\rho U [\![\mathscr{E}]\!] - [\![V_i t_i]\!] + [\![q_i n_i]\!] = 0, \tag{3.6c}$$

which express conservation of mass, momentum and energy, respectively. Here $\mathbf{V}$ is the particle velocity, U the boundary propagation velocity relative to the external medium, $\hat{n}$ the normal to the boundary, $\mathbf{t}$ the traction, $\mathscr{E}$ the total energy density and $\mathbf{q}$ the heat flux.

From the first and second conditions, it is clear that the normal components of velocity and tractions are continuous. Burridge (1976) assumes that the tractions vanish at the surface of the failure zone; this is a sufficient but not necessary condition which is equivalent to

$$[\![t_i]\!] = [\![V_i]\!] = 0 \tag{3.7a}$$

$$\rho U [\![\mathscr{E}]\!] + [\![q_i n_i]\!] = 0. \tag{3.7b}$$

In other words, the jump in energy density is balanced by the jump in the normal heat flux. This is the boundary condition for Stefan's problem. If we consider the case of a rapid growth of the failure zone, whereby heat conduction terms may be neglected, (3.7) reduces to

$$[\![\mathscr{E}]\!] = [\![u]\!] + \tfrac{1}{2}[\![V_k V_k]\!] = 0, \tag{3.8}$$

where u is the internal energy density. From (3.7a) it is seen that $[\![u]\!]$ vanishes, which means that the change in u due to disordering of the material upon failure is exactly compensated by the loss in strain energy density. While this boundary condition represents a rather specialized case, it is instructive to compare the exact solution obtained in that case by Burridge (1975) with our 'transparent' solution. This was done by Burridge in the spectral domain, with the conclusion that the difference is relatively minor and lies mainly in the high frequency, fine structure of the spectra.

Fig. 2 is a comparison of our time domain solution with Burridge's. The parameters are

$$V_p = \sqrt{3} V_s, \quad V_R = 0.5 V_s, \quad r = 20R(\tau),$$

and the waveforms are plotted as a function of the dimensionless time $(t - r/V_p)(V_s/R_0)$. Several phases are indicated on the figure. They are the phases P, S, P_s, S_s, P'_s, S'_s described earlier and P'_{sd}, S'_{sd}, the stopping phases radiated from the far side of the cavity, assuming that they must propagate around the cavity (diffracted arrivals). Comparison of the two solutions is rather favourable. Rise times and amplitudes are in good agreement for both P and S pulses. The main differences appear in the pulse widths which are smaller for our solution, since the phases P'_s and S'_s arrive too early, and in the oscillations following the main pulses. Burridge (1975) showed that these oscillations are due to the excitation of three free spheroidal modes of oscillation of the cavity, with angular order 2. The same differences appear in the far-field terms as well, as illustrated in Fig. 3.

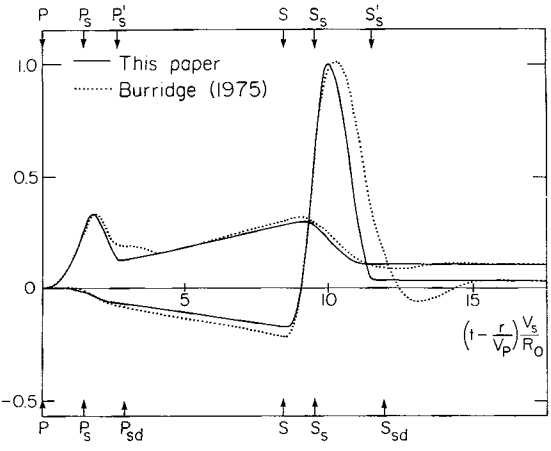

Figure 2. Comparison of the 'transparent source' solution used in this paper with an exact solution (Burridge 1975).

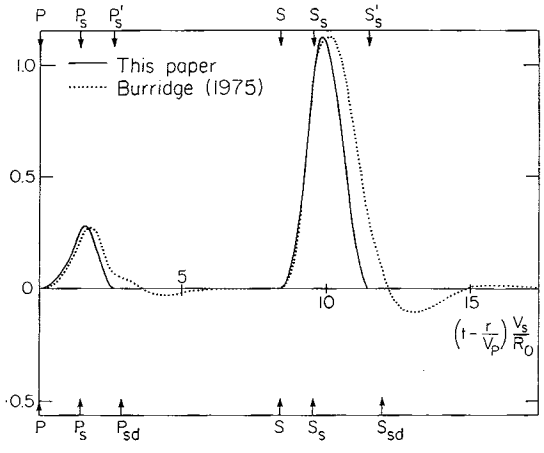

Figure 3. Same as Fig. 2; far-field terms only.

Based on these comparisons, it appears that the main shortcoming of the 'transparent' approximation is that it yields slightly narrowed pulses. One expects that the effect is largely controlled by the geometry of the failure zone, the spherical case being rather unfavourable. For other geometries, for which exact solutions to the stress relaxation problem are untractable, this approximation should offer significant simplifications, while yielding adequate results for most purposes. The main advantage of the transparent solution (1.1a) lies in the fact that it only depends on $\mathbf{u}^*(t_0)$, the initial value field; this means that one only has to solve a sequence of static equilibrium problems instead of a complete dynamic problem, whether the solution is obtained analytically or numerically.

3.3 EFFECTS OF GROWTH HISTORY

For the purpose of illustrating the effect of a more complicated growth history of the cavity, the results of selected calculations are shown in Figs 4–6. In all three cases the parameters

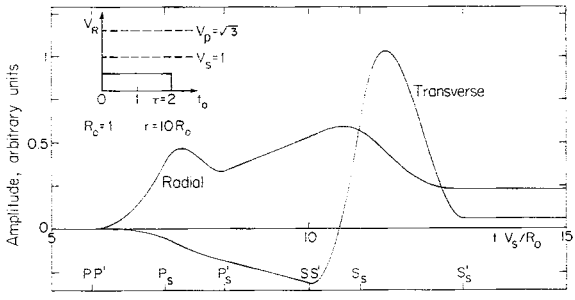

Figure 4. Near-field waveforms at 10 cavity radii. Cases of constant subsonic rupture velocity. Parameters are given in the text.

are, in arbitrary units

$$V_p = \sqrt{3}, \quad V_s = 1, \quad R_0 = 1, \quad \tau = 2, \quad r = 10R_0.$$

Fig. 4 exhibits the displacement pulses for the case of a constant ($V_R = \dot{R} = 0.5$) rupture velocity. We know that in this case the far-field pulses have an emergent, parabolic onset (e.g. Minster & Suteau 1977). The onsets of the P and S pulses on Fig. 4 also exhibit this emergent character. Fig. 5 corresponds to the case of a rupture velocity V_R decreasing linearly from V_s to zero so that the total duration takes the same value. The main contrast with Fig. 4 appears in a shorter rise time of the radial pulse and a sharp onset of the transverse pulse. In Fig. 6, the rupture velocity was assumed to keep the supersonic value

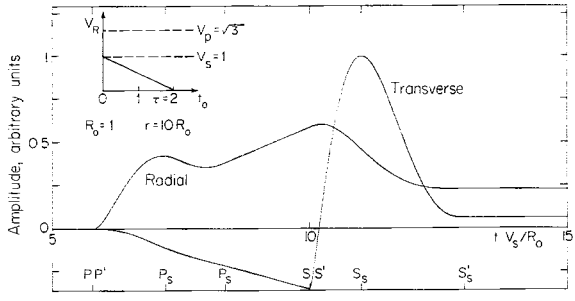

Figure 5. Same as Fig. 4. Case of linearly decreasing, subsonic rupture velocity. Parameters are given in the text.

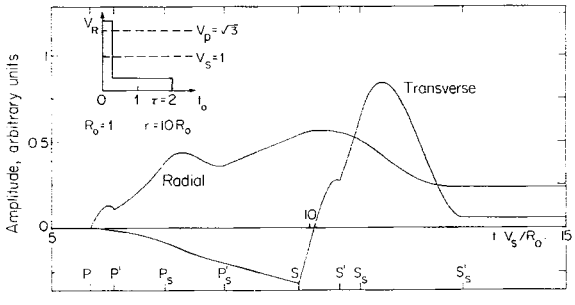

Figure 6. Same as Fig. 4. Case of discontinuous, supersonic and then subsonic rupture velocity. Parameters are given in the text.

$V_R = 2$ until $\tau_p = 0.2$, after which $V_R = 1/3$ for $0.2 = \tau_p \leqslant t_0 \leqslant \tau = 2$. Because the phenomenon involves an interval of supersonic growth of the cavity, the phases P and S occur at

$$t_p = \frac{r - R(\tau_p)}{V_p} + \tau_p, \tag{3.9}$$

$$t_s = \frac{r - R(\tau_s)}{V_s} + \tau_s, \tag{3.10}$$

where $\tau_s = \tau_p$ in that case (*cf.* Minster & Suteau 1977). In addition, the interval of supersonic growth gives rise to incident parabolic onsets of the far-field pulses; this behaviour is also evident in the near-field pulses of Fig. 6.

It is noteworthy that the most obvious differences between the three cases just described occur mainly in the 'P' and 'S' pulses. The portions of these waveforms which are exclusively composed of near-field terms (posterior to P_s' on the radial component; anterior to S on the transverse component) undergo only moderate modifications. In other words, near-field terms appear to be only mildly sensitive to the growth history of the source. Heuristically, this might be attributed to the rapid decay with distance of these terms, so that they are mostly sensitive to the final stages of the phenomenon, and in particular to the final static configuration of the source. This is certainly true of the static displacements (posterior to S_s').

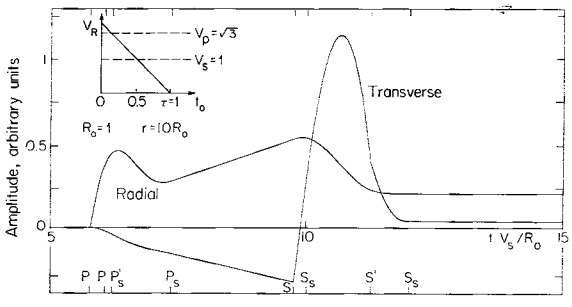

Figure 7. Near-field waveforms at 10 cavity radii. Case of linearly decreasing rupture velocity from a supersonic initial value to zero.

Finally, we show, in Fig. 7, the waveforms corresponding to a linearly decreasing rupture velocity, from a supersonic initial value of 2 to a final value of 0. All three regimes – supersonic, transonic, subsonic – are therefore represented and the eight phases listed in the first section are all distinct. It is interesting to note that only the phases P, S and, to a lesser extent, S_s are visible in the waveforms. The reason is that, as opposed to Fig. 6, the rupture velocity is a continuous function of time in this case. A similar observation also holds in the far field (Minster & Suteau 1977).

Conclusions

The main conclusions of this study are threefold.

(1) Use of a transparent source approximation leads to considerable simplification of the near-field radiation problem. Even in the geometrically unfavourable case of a spherical failure zone, the waveforms compare favourably with exact solutions in cases where the latter are available.

(2) The simpler algebraic form of the solution makes it possible to consider more complex growth histories of the source, but it appears that near-field contributions to the radiation field are relatively insensitive to the detailed variation of the rupture velocity, at least in the class of sources considered here.

(3) Finally, time domain moment estimators at close range are less contaminated by near-field effects for the S wave than they are for the P wave. Therefore, analysis of the transverse pulse on near-field accelerograms will generally yield a better picture of the source.

Acknowledgments

This research was supported by the Advanced Research Projects Agency of the Department of Defense, and was monitored by the Air Force Office of Scientific Research under Contract No. F49620-77-C-0022. Contribution No. 3021, Division of Geological and Planetary Sciences, California Institute of Technology, Pasadena, California 91125, USA.

References

Archambeau, C. B., 1968. General theory of elastodynamic source fields, *Rev. Geophys.*, **6**, 241–288.

Archambeau, C. B., 1972. The theory of stress wave radiation from explosions in prestressed media, *Geophys. J. R. astr. Soc.*, **29**, 329–366.

Archambeau, C. B. & Minster, J. B., 1978. Dynamics in prestressed media with moving phase boundaries: a continuum theory of failure in solids, *Geophys. J. R. astr. Soc.*, **52**, 65–96.

Burridge, R., 1975. The pulse shapes and spectra of elastic waves generated when a cavity expands in an initial shear field, *J. geophys. Res.*, **80**, 2606–2607.

Burridge, R., 1976. Reply, *J. geophys. Res.*, **81**, 1037–1038.

Harkrider, D. G., 1976. Potentials and displacements for two theoretical seismic sources, *Geophys. J. R. astr. Soc.*, **47**, 97–133.

Harkrider, D. G., 1977. Elastic relaxation coefficients for a spherical cavity in a prestressed medium of arbitrary orientation, *Geophys. J. R. astr. Soc.*, **50**, 487–491.

Koyama, J., Horiuchi, S. E. & Hirasawa, T., 1973. Elastic waves generated from sudden vanishing of rigidity in a spherical region, *J. Phys. Earth*, **21**, 213–226.

Minster, J. B., 1973. Elastodynamics of failure in a continuum, *PhD thesis*, California Institute of Technology, Pasadena.

Minster, J. B. & Suteau, A. M., 1977. Far-field waveforms from an arbitrary expanding, transparent spherical cavity in a prestressed medium, *Geophys. J. R. astr. Soc.*, **50**, 215–233.

Ohnaka, M., 1973. A physical understanding of the earthquake source mechanism, *J. Phys. Earth*, **21**, 39–59.

Pendse, C. G., 1948. On the analysis of a small arbitrary disturbance in a homogeneous isotropic elastic solid, *Phil. Mag. Ser. 7*, **39**, 862–867.

Randall, M. J., 1964. On the mechanism of earthquakes, *Bull. seism. Soc. Am.*, **54**, 1283–1289.

Randall, J. M., 1973a. Spectral peaks and earthquakes source dimension, *J. geophys. Res.*, **78**, 2609–2611.

Randall, J. M., 1973b. Low frequency spectra in seismic waves from explosions, *Geophys. J. R. astr. Soc.*, **32**, 387–388.

Snoke, J. A., 1976. Implications of moving boundaries in elastodynamics, Comments on 'the pulse shapes and spectra of elastic waves generated when a cavity expands in an initial shear field' by Robert Burridge, *J. geophys. Res.*, **81**, 1035–1036.

Appendix A: evaluation of the potentials

By decomposition of the spherical Bessel function according to

$$j_1(z) = \tfrac{1}{2}\,[h_1^{(1)}(z) + h_1^{(2)}(z)], \qquad \text{(A.1)}$$

the integrand in (1.7) may be written:

$$I_\alpha(t_0) = \int_{-\infty}^{+\infty} \frac{3\dot{R}_\alpha(t_0)}{4\pi V_\alpha} \left\{ \left(-\frac{i}{k_\alpha r} - \frac{3}{k_\alpha^2 r^2} + \frac{3i}{k_\alpha^3 r^3} \right) \left(-1 - \frac{i}{k_\alpha R(t_0)} \right) \right.$$
$$\times \exp\left(ik_\alpha [V_\alpha(t-t_0) - r + R(t_0)]\right) + \left(-\frac{i}{k_\alpha r} - \frac{3}{k_\alpha^2 r^2} + \frac{3i}{k_\alpha^3 r^3} \right) \left(-1 + \frac{i}{k_\alpha R(t_0)} \right)$$
$$\left. \times \exp\left(ik_\alpha [V_\alpha(t-t_0) - r - R(t_0)]\right) - \frac{2iR^2(t_0)}{k_\alpha r^3} \exp\left[ik_\alpha V_\alpha(t-t_0)\right] \right\} d\omega, \qquad \text{(A2)}$$

or

$$I_\alpha(t_0) = I_\alpha^{(1)}(t_0) + I_\alpha^{(2)}(t_0) + I_\alpha^{(3)}(t_0). \qquad \text{(A.3)}$$

Because of the poles occurring at $\omega = 0$, we define the values of these integrals by

$$\int_{-\infty}^{+\infty} = \lim_{x \to \infty} \int_{-x}^{+x} \qquad \text{(A4)}$$

The geometry in the complex ω plane is described on Fig. (A.1). We have

$$\int_{-x}^{+x} = \frac{1}{2}\left[\int_A + \int_B\right] = -\frac{1}{2}\left[\int_{C_1} + \int_{C_2}\right]. \qquad \text{(A.5)}$$

In the limit of $x \to \infty$ one must deform the contours C_1 and C_2 into the upper half plane or the lower half plane according to the signs of the real parts of the exponents in (A.2). Let R_1, R_2, R_3 be the residues of the three integrands at the origin, and define

$$t' = t - r/V_\alpha, \qquad \text{(A.6)}$$

$$\rho = V_\alpha(t' - t_0), \qquad \text{(A.7)}$$

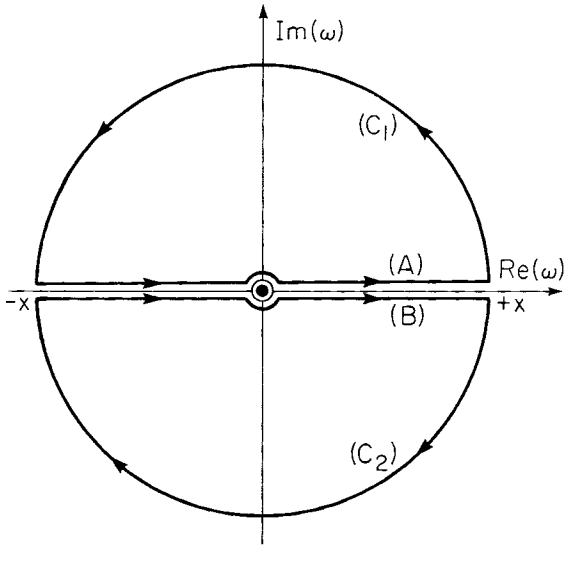

Figure (A.1).

then, for $0 < t_0 < \tau < t$,

$$R_1 = \frac{3i\dot{R}_\alpha(t_0)}{4\pi}\left[-\frac{\rho}{rR}+\frac{3R}{2r^2}-\frac{3\rho^2}{2r^2R}+\frac{3\rho R}{2r^3}+\frac{R^2}{r^3}-\frac{\rho^3}{3r^3R}\right], \tag{A.8}$$

$$R_2 = \frac{3iR_\alpha(t_0)}{4\pi}\left[\frac{\rho}{rR}-\frac{3R}{2r^2}+\frac{3\rho^2}{2r^2R}-\frac{3\rho R}{2r^3}-\frac{R^2}{r^3}+\frac{\rho^3}{3r^3R}\right], \tag{A.9}$$

$$R_3 = -\frac{3i\dot{R}_\alpha(t_0)R^2}{2\pi r^3}. \tag{A.10}$$

We must now distinguish three cases, depending on the value of t_0. Define the times τ_1 and τ_2 by

$$\left.\begin{aligned} V_\alpha(t'-\tau_1)-R(\tau_1)&=0,\\ V_\alpha(t'-\tau_2)+R(\tau_2)&=0.\end{aligned}\right\} \tag{A.11}$$

We have

(a) $t_0 < \tau_1$,

then

$\rho - R > 0$

and

$$I_\alpha(t_0) = 2i\pi\,[R_1+R_2+R_3] = 0. \tag{A.12}$$

(b) $\tau_1 < t_0 < \tau_2$,

then

$\rho - R < 0 < \rho + R$

and

$$I_\alpha(t_0) = 2i\pi\,[R_1-R_2+R_3]$$

$$= -\frac{3\dot{R}_\alpha}{4}\left[-\frac{2\rho}{rR}+\frac{3R}{r^2}-\frac{3\rho^2}{r^2R}+\frac{3\rho R}{r^3}-\frac{\rho^3}{r^3R}-\frac{2R^2}{r^3}\right]. \tag{A.13}$$

(c) $\tau_1 < \tau_2 < t_0$,

then

$\rho + R < 0$

and

$$I_\alpha(t_0) = 2i\pi\,[-R_1-R_2+R_3] = \frac{3R^2\dot{R}_\alpha}{r^3}. \tag{A.14}$$

In addition, one must subtract the final static term $(R(\tau)/r)^3$ from the result since it is no part of the radiation field. This proves equations (1.8) to (1.17) of the text.

Appendix B: evaluation of the integrals $J_1 \ldots J_7$ and their radial derivatives

We assume a quadratic growth of the cavity radius of the form

$$\left.\begin{aligned} R(t_0) &= \frac{A}{2}(t_0 - z_1)(t_0 - z_2), \\ R(t_0) &= at_0^2 + bt_0 + c. \end{aligned}\right\} \tag{B.1}$$

A is non-positive, and in equations (1.9) to (1.15) of the text we have

$$z_2 \leqslant T_i \leqslant T_f \leqslant z_1. \tag{B.2}$$

The integrals J_1 to J_7 may then be evaluated analytically using straightforward integration by parts and changes of variables. We get

$$J_1 = (t' - z_2)\ln\frac{T_f - z_2}{T_i - z_2} + (t' - z_1)\ln\frac{z_1 - T_f}{z_1 - T_i} - 2(T_f - T_i) + \frac{t' - \tau_\alpha}{3}H(\tau_\alpha - T_i)H(T_f - \tau_\alpha), \tag{B.3}$$

$$J_2 = \frac{1}{2}[R^2(T_f) - R^2(T_i)] + \frac{R^2(\tau_\alpha)}{3}H(\tau_\alpha - T_i)H(T_f - \tau_\alpha), \tag{B.4}$$

$$J_3 = (t' - z_2)^2\ln\frac{T_f - z_2}{T_i - z_2} + (t' - z_1)^2\ln\frac{z_1 - T_f}{z_1 - T_i} + (T_f - T_i)(T_f + T_i + z_1 + z_2 - 4t') + \frac{(t' - \tau_\alpha)^2}{3}H(\tau_\alpha - T_i)H(T_f - \tau_\alpha), \tag{B.5}$$

$$J_4 = -\frac{2a^2}{5}(T_f^5 - T_i^5) + \left(\frac{a^2 t'}{2} - \frac{3ab}{4}\right)(T_f^4 - T_i^4) + \left(abt' - \frac{b^2 + 2ac}{3}\right)(T_f^3 - T_i^3) + \left(\frac{b^2 + 2ac}{2}t' - \frac{bc}{2}\right)(T_f^2 - T_i^2) + bct'(T_f - T_i) + \frac{(t' - \tau_\alpha)R^2(\tau_\alpha)}{3}H(\tau_\alpha - T_i)H(T_f - \tau_\alpha), \tag{B.6}$$

$$J_5 = (t' - z_2)^3\ln\frac{T_f - z_2}{T_i - z_2} + (t' - z_1)^3\ln\frac{z_1 - T_f}{z_1 - T_i} - \frac{3}{2}(T_f - T_i)[(t' - T_f)^2 + (t' - T_i)^2 + (t' - z_1)^2 + (t' - z_2)^2] + \frac{1}{4}(T_f - T_i)[(T_f - z_1)^2 + (T_f - z_2)^2 + (T_i - z_1)^2 + (T_i - z_2)^2] + \frac{1}{3}(T_f - T_i)^3 + \frac{(t' - \tau_\alpha)^3}{3}H(\tau_\alpha - T_i)H(T_f - \tau_\alpha), \tag{B.7}$$

$$J_6 = \frac{1}{3}[R^3(T_f) - R^3(T_i)] + \frac{R^3(\tau_\alpha)}{3}H(\tau_\alpha - T_i)H(T_f - \tau_\alpha), \tag{B.8}$$

$$J_7 = \frac{R^3(\tau)}{3} - \frac{R^3(T_f)}{3} + \frac{R^3(\tau_\alpha)}{3}H(\tau_\alpha - T_f)H(\tau - \tau_\alpha). \tag{B.9}$$

In order to obtain the accelerations by equation (3.3), we also need the radial derivatives of these integrals. Using

$$\left.\begin{aligned} t' - T_f &= -R(T_f)/V_\alpha, \\ t' - T_i &= R(T_i)/V_\alpha, \end{aligned}\right\} \tag{B.10}$$

and, by differentiation of (1.17)

$$\frac{dT_f}{dr} = \frac{-1}{V_\alpha - \dot{R}(T_f)}; \quad \frac{dT_i}{dr} = \frac{-1}{V_\alpha + \dot{R}(T_i)}, \tag{B.11}$$

we can compute these derivatives. After some algebra, one finds

$$\begin{aligned} \frac{\partial I_\alpha}{\partial r} = &-\frac{\delta(T_i - \tau_\alpha)}{2r} - \frac{3}{2r}\left(\ln\frac{R(T_f)}{R(T_i)} + \dot{R}(T_f)\frac{dT_f}{dr} + \dot{R}(T_i)\frac{dT_i}{dr}\right) \\ &- \frac{6V_\alpha}{r^2} J_1 + \frac{27}{4r^3} J_2 - \frac{27}{4r^3} V_\alpha^2 J_3 + \frac{27V_\alpha}{4r^4} J_4 - \frac{9V_\alpha^3}{4r^4} J_5 - \frac{9}{2r^4} J_6 - \frac{9}{r^4} J_7 \\ &+ \frac{3R^3(\tau)}{r^4} - \frac{R^3(\tau_\alpha)}{r^4}\delta(\tau_\alpha - T_f)\frac{dT_f}{dr}. \end{aligned} \tag{B.12}$$

However, this expression exhibits singularities in some cases (e.g. when $R(t_0) = At_0^2 + V_\alpha t_0$), and is rather delicate to use in numerical calculations. For that reason, it is preferable to use the procedure described in the text to obtain the velocities.